Supplementary Information

Purely Organic 4HCB Single Crystal Exhibiting High Hole Mobility for Direct Detection of Ultralow-Dose X-Radiation

Dou Zhao[1], Meng Xu[1], Bao Xiao[1], Binbin Zhang[1], Lei Yan[2], Guoqiang Zeng[2], Alain Dubois[1,3], Paul Sellin[4], Wanqi Jie[1], and Yadong Xu[1]*

[1]Key Laboratory of Radiation Detection Materials and Devices, Ministry of Industry and Information Technology, School of Materials Science and Engineering & State Key Laboratory of Solidification Processing, Northwestern Polytechnical University, Xi'an, Shaanxi 710072, China.

[2]Nuclear Technology Key Laboratory of Earth Science, Chengdu University of Technology, Chengdu, 610051, China.

[3]Laboratory of Physical Chemistry - Matter and Radiation, Sorbonne Universite, France.

[4]Department of Physics, University of Surrey, UK.

*Correspondence: xyd220@nwpu.edu.cn,

Supplementary Discussion 1

Calculation of signal-to-noise ratio (SNR)[1]

The signal current (I_{signal}) was derived by subtracting the average photocurrent (I_{photo}) by the average dark current (I_{dark}). The noise current (I_{noise}) was obtained by calculating the standard deviation of the photocurrent.

$$I_{signal} = \bar{I}_{photo} - \bar{I}_{dark} \tag{S1}$$

$$I_{noise} = \sqrt{\frac{1}{N}\sum_{1}^{N}(I_i - \bar{I}_{photo})} \tag{S2}$$

Then the signal-to-noise ratio (SNR) was calculated as

$$SNR = I_{signal}/I_{noise} \tag{S3}$$

As an example, for 4HCB *SC* device at 600 V/cm and under 0.2875 $\mu Gy_{air}\ s^{-1}$, the calculated average photocurrent, dark current, and noise current was 0.4398 pA, 0.1132 pA, and 0.0209 pA, respectively, resulting in a *SNR* value of 15.62.

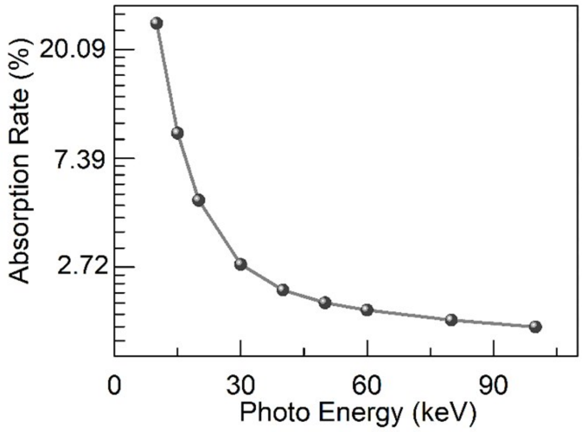

Supplementary Figure 1. Attenuation efficiency (φ%) of the 4HCB single crystal (thickness 1mm) to versus X-ray photos energy.

Attenuation efficiency is calculated by:

$$\varphi = 1 - exp(-R \times d) \tag{S4}$$

where R is the photon absorption (cm^{-1}) of 4HCB, $R = R_m \times g$, R_m is total attenuation coefficient (cm^2/g), obtained by photo cross-section database (XCOM)[2], g is mass density (g/cm^3), d=0.1 cm.

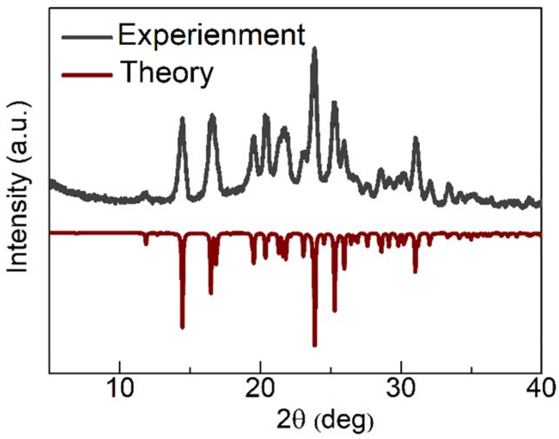

Supplementary Figure 2. The Powder XRD pattern of as-grown 4HCB single crystal. The Powder X-ray Diffraction (PXRD) patterns of the as-grown crystal was compared with the simulated one. Almost no difference existed between experimental and simulated patterns, confirming the absence of solvent incorporation into the crystallographic lattice and high purity of as-grown crystals.

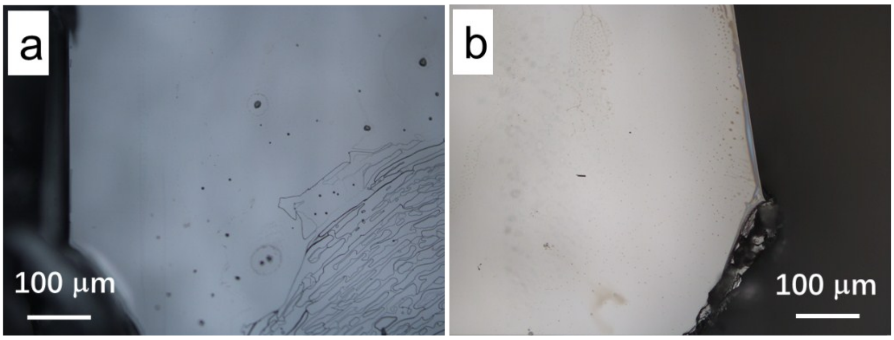

Supplementary Figure 3. Surface charaterization of crystals obtained at different growth temperatures (a) 5 °C, (b) -5 °C. We can observe that there are fewer layered defects or pits on the surface of crystals obtained at -5 ℃ (slower growth rate), indicating a higher crystal quality at the lower growth rate.

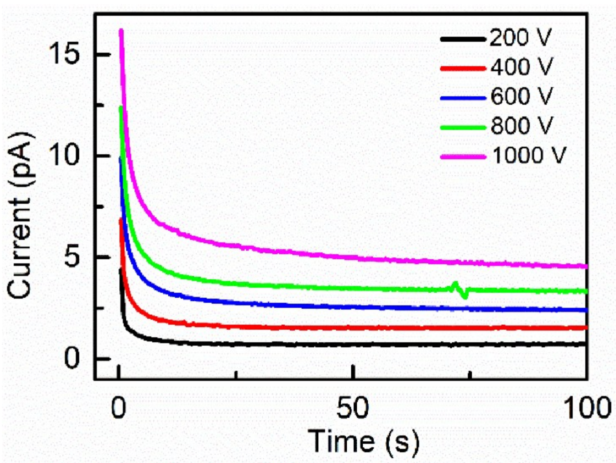

Supplementary Figure 4. Leakage current-time (I-T) curve at various bias voltages. The steady resistivity of post-surface treated crystals was calculated by leakage current-time relations at changing bias voltages. The values of current (I) at the range of 80 to 100 seconds were used for calculation.

$$\rho = \frac{I\,d}{AU} \tag{S5}$$

where A is the area of electrode, d is the thickness of the crystals, and U is the bias voltages.

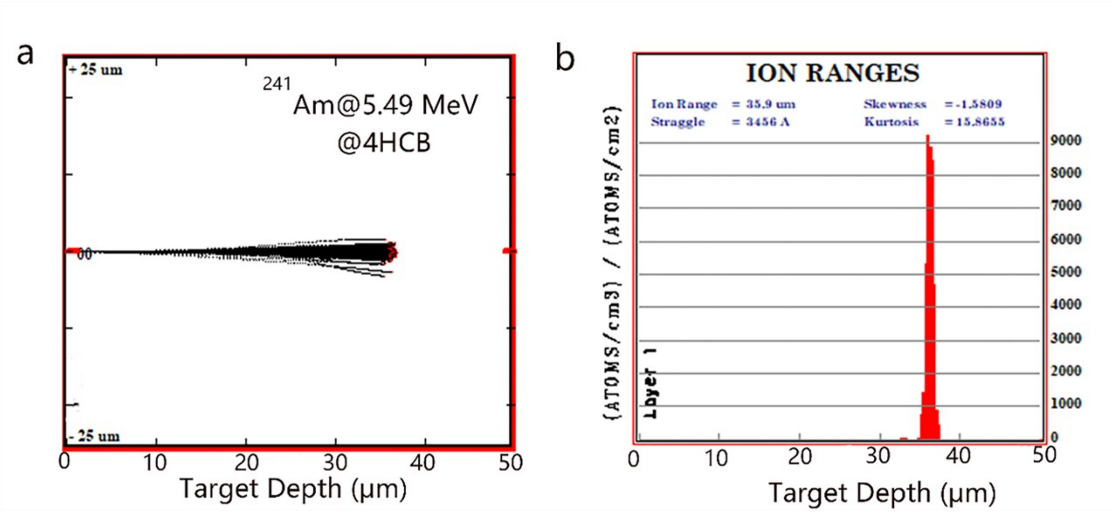

Supplementary Figure 5. (a) Simulation of penetration depth of alpha particle 4HCB detector by 500 alpha particles (b) Ion ranges of these alpha 500 particles in the 4HCB detector. By using SRIM software, the penetration depth of alpha particle 4HCB detector was simulated to be 35.9 μm by a @5.49MeV 241Am alpha source.

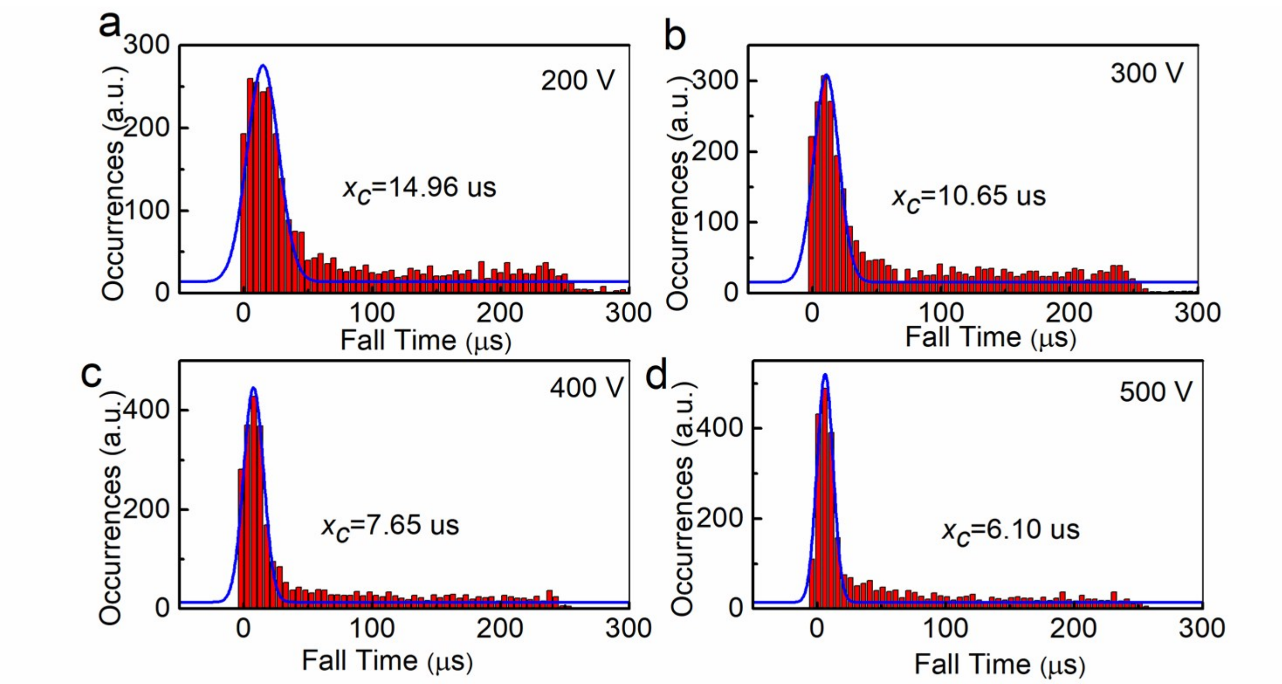

Supplementary Figure 6. Histogram statistics of fall time, (a)~(d) biased at 200-500 V.

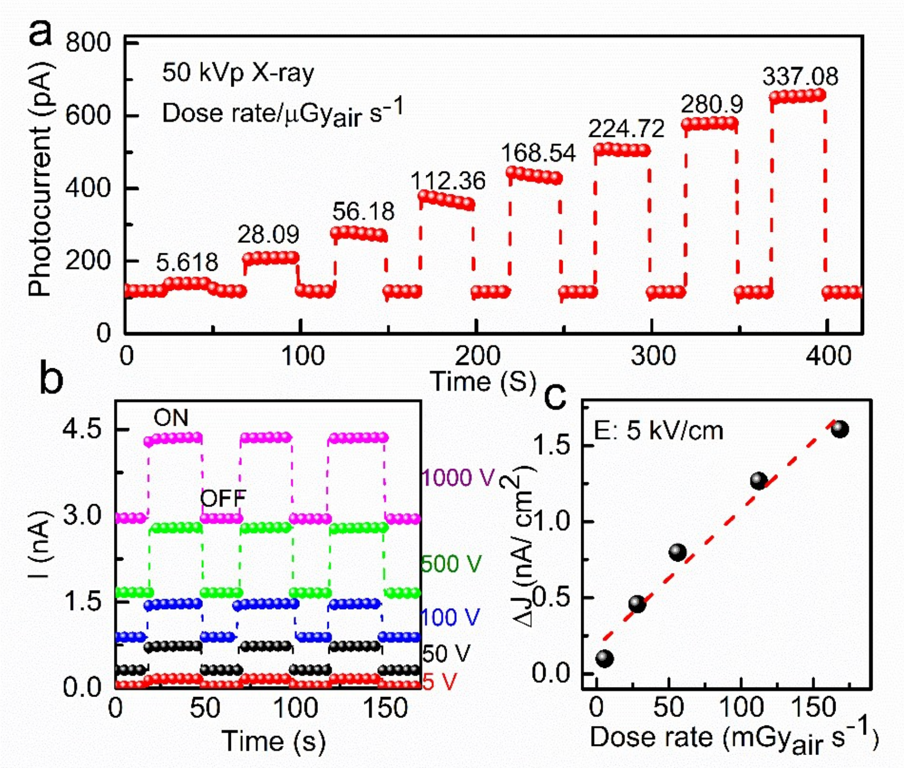

Supplementary Figure 7. (a) *I-T* curves of devices based on as-grown crystals with increasing dose rate, (b) X-ray induced Photocurrent-Time (*I-T*) curve at different bias voltage (*V*) under high Dose rate 830 μGy$_{air}$ s^{-1}, (c) Photocurrent density (*ΔJ*) reported as a function of Dose rate (*D*) (with blue dots) and linear fitting curve (with red dashed line) at 5.0 kV/cm.

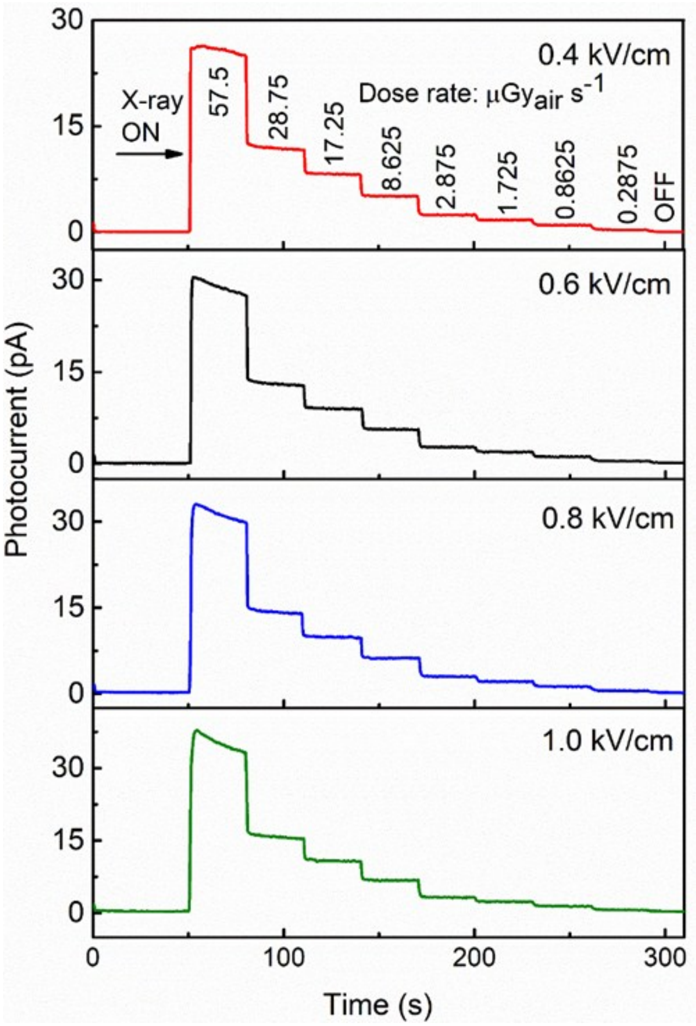

Supplementary Figure 8. I-T curves of devices based on polished crystals at various electric field.

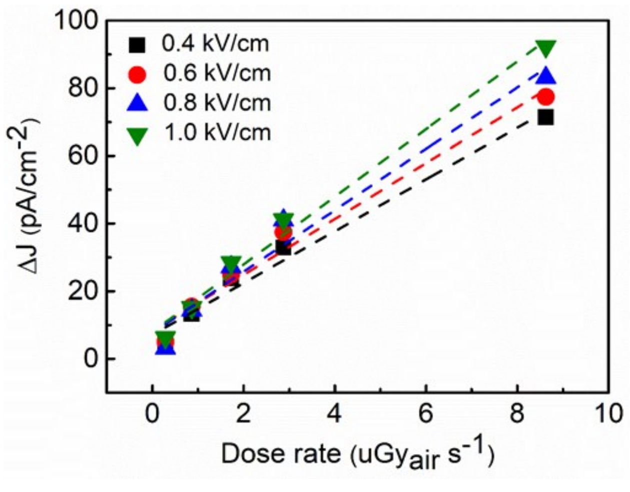

Supplementary Figure 9. I-T curves of devices based on polished crystals at various electric field.

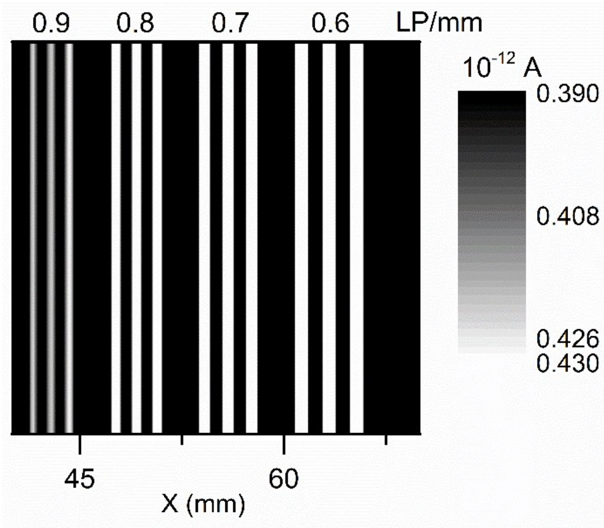

Supplementary Figure 10. X-ray imaging of the sharp edge of the line pair card. Under exposure of 50 kVp X-ray (dose rate: around 150 uGy_{air} s^{-1}). For acquiring X-ray imaging, the object was adhered on a x-y scanning stage, and we controlled the object to transport in the directions along x and y axis.

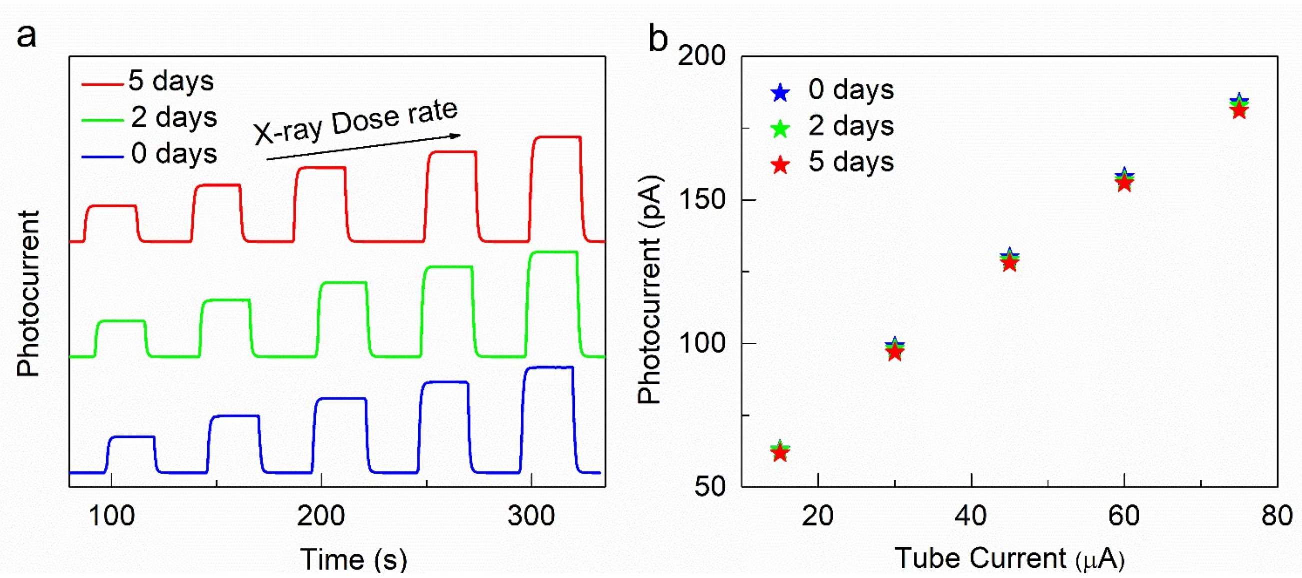

Supplementary Figure 11. Long-time stability measurements of 4HCB detectors after devices fabrication 0 days, 2 days and 5 days, (a) on-off curves, (b) photocurrent vs. X-ray dose rate (adjusting by Tube current).

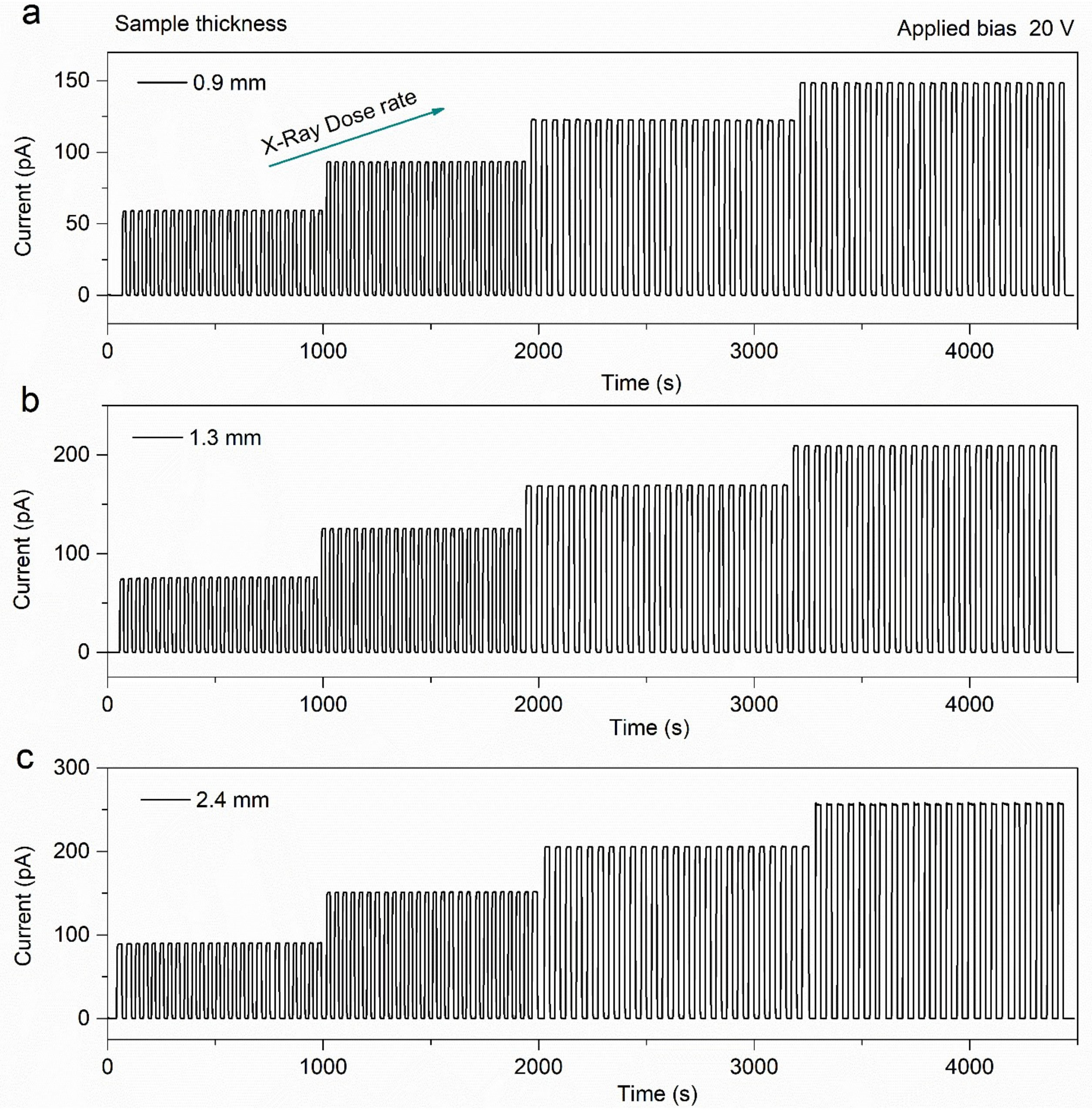

Supplementary Figure 12. Long-time X-ray response of 4HCB detectors with thickness of (a) 0.9 mm, (b) 1.3 mm, (c) 2.4 mm, under bias of 20 V (25 on-off cycles for each X-ray dose rate).

Reference

1. W. Pan, H. Wu, J. Luo, Z. Deng, C. Ge, C. Chen, X. Jiang, W.-J. Yin, G. Niu and L. Zhu, *Nat. Photon.*, 2017, **11**, 726.
2. M. Berger, *http://physics. nist. gov/PhysRefData/Xcom/Text/XCOM. html*, 1998.